

HD-Bind: Encoding of Molecular Structure with Low Precision, Hyperdimensional Binary Representations

Derek Jones^{1,2}, Jonathan E. Allen¹, Xiaohua
Zhang³, Behnam Khaleghi¹, Jaeyoung Kang¹, Weihong
Xu¹, Niema Moshiri¹ and Tajana S. Rosing¹

¹Department of Computer Science and Engineering, University of
California - San Diego, La Jolla, CA.

²Global Security Computing Applications Division, Lawrence
Livermore National Laboratory, Livermore, CA.

³Biosciences and Biotechnology Division, Lawrence Livermore
National Laboratory, Livermore, CA.

Contributing authors: wdjones@ucsd.edu; allen99@llnl.gov;
tajana@ucsd.edu;

Abstract

Purpose: Publicly available collections of drug-like molecules have grown to comprise 10s of billions of possibilities in recent history due to advances in chemical synthesis (i.e. combinatorial chemistry). Traditional methods for identifying “hit” molecules from a large collection of potential drug-like candidates have relied on biophysical theory to compute approximations to the Gibbs free energy of the binding interaction between the drug to its protein target. A major drawback of the approaches are that they require exceptional computing capabilities to consider for even relatively small collections of molecules. **Methods:** Hyperdimensional Computing (HDC) is a recently proposed learning paradigm that is able to leverage low-precision binary vector arithmetic to build efficient representations of the data that can be obtained without the need for gradient-based optimization approaches that are required in many conventional machine learning and deep learning approaches. This algorithmic simplicity allows for acceleration in hardware that has been previously demonstrated for a range

of application areas. We consider existing HDC approaches for molecular property classification and introduce two novel encoding algorithms that leverage the extended connectivity fingerprint (ECFP) algorithm.

Results: We show that HDC-based inference methods are as much as $90 \times$ more efficient than more complex representative machine learning methods, and achieve an acceleration of nearly 9 orders of magnitude as compared to inference with molecular docking. We also show that HDC-methods implemented in a variety of tools can match competitive performance in terms of training with respect to simple baseline ML models while retaining competitive predictive performance on a number of tasks ranging from well-studied benchmarks such as MoleculeNet molecular property prediction tasks as well as the DUD-E and LIT-PCBA bind/no-bind activity classification datasets.

Conclusions: We demonstrate multiple approaches for the encoding of molecular data for HDC and examine their relative performance on a range of challenging molecular property prediction and drug-protein binding classification tasks. Our work thus motivates further investigation into molecular representation learning to develop ultra-efficient pre-screening tools.

Keywords: Machine Learning, Kernel Methods, Hyperdimensional Computing, Computational Chemistry, Drug Discovery

1 Introduction

The modern drug discovery process consists of multiple sequential steps that progress from an initial large collection of candidates sampled from the intractable drug-like chemical space. These candidates are filtered according to their likelihood of success according to some *scoring function*. The results of this *virtual screen* are used to identify chemical “leads” for more rigorous yet expensive experimental validation. To consider all hypothetical possible candidate drug molecules for activity with a *single* protein target would require approximately 3.12×10^{34} years to search with brute force[1], assuming a throughput of approximately $10^{60}/10^{18}$ molecules per second (for the sake of simplicity, one molecule per FLOP) with current generation exascale leadership-class computing facilities. Clearly even with this generous estimate, replicating this effort for all known 10s of thousands human proteins with experimentally-determined crystal structures would require computing resources that are not expected to be generally available in our lifetimes. In practice, collections of purchasable drug-like molecules are on the order of billions of possibilities. Even with this constraint on chemical space, current scoring functions for inferring protein-drug interactions still require high performance computing (HPC) resources to conduct screens on the scale of billions in an acceptable time frame [2].

Scoring functions are roughly divided into the distinct categories of physics-based and machine learning-based. Physics-based methods such as the *molecular docking* methods [3, 4] are generally believed to be on the “fast” end of the spectrum of accuracy versus latency tradeoff. More accurate methods including Molecular Mechanics/Generalized Boltzmann Surface Area (MM/GBSA)[5, 6] which is used to “re-score” docking poses and update their rankings or binding free-energy calculations based upon intensive atomistic molecular dynamics (MD) simulations, are infeasible to run for even a relatively small number of candidate possibilities [4, 7]. A general workflow then is to first apply the cheaper docking methods followed by more expensive but accurate calculations based on MD simulations[8]. Current research is attempting to use machine learning to produce efficient surrogate models of physics-based calculations [9, 10].

Much interest in the drug discovery community has shifted towards the development of deep learning models for prediction of protein-ligand interactions, with competitive results on experimental datasets such as PDBBind[11–13]. Although such methods are highly efficient as compared to traditional physics-based calculations, deploying these methods in practice on billions of molecules requires significant compute resources[8, 11, 14, 15]. It is also well known that deep learning models are incredibly complex in their architecture definitions as well as their training requirements as compared to more traditional machine learning approaches such as kernel methods. While gradient based optimization does allow for Deep Learning models to handle processing much larger datasets than kernel methods are practically capable of, deep learning models are also notoriously complex architectures, so much so that an entire area of research is dedicated towards their acceleration both at the algorithm level and in hardware. Ultimately scaling these models to address scoring growing collections of molecules will depend on success in development of specialized hardware that can also keep pace with the rapid level of model development.

Hyper-dimensional computing (HDC) is an emerging paradigm of lightweight machine learning with parallels to kernel methods [16–20]. In a simple description, HDC requires the specification of an *encoding* method to transform the raw input data to a high-dimensional vector space as *hypervectors*. Given a notion of similarity metric defined on the high-dimensional space, such as cosine similarity which is only sensitive to the relative orientation, the hypervectors can be aggregated in order to build canonical class representations, forming the *associative memory* of the model. Inference then simply requires computing similarity between the query point with the elements of the associative memory (one for each class). Thus, HDC has been studied in the computer hardware community for some time in parallel to more traditional deep learning research as it provides the ability to receive massive speedups at the hardware level[19, 21–26].

Despite the potential of HDC in the context of screening protein-ligand interactions, to the best of our knowledge there has only been a single previously reported study of HDC on a molecular machine learning task in general [27]. In our work, we seek to expand upon previous work by considering additional structure-based encoding methods derived from extended connectivity fingerprints (ECFP), a widely used representation in a range of molecular modeling tasks and similarity analysis [28], as well as Self-referencing embedded strings (SELFIES)[29]. We evaluate on MoleculeNet in order to facilitate our comparison to previously reported state of the art results. We then seek to establish a rigorous analysis of HDC-based screening models in the context of publicly available collections of labeled molecules frequently studied in ML-based approaches.

The potential for HDC to serve as a lightweight, readily available screening technique that is particularly amenable to advances in hardware architecture, can thus provide a crucially important tool for efficient screening of increasingly large collections of molecular representations.

2 Results

2.1 Comparing to previous work through MoleculeNet

To sanity-check our methods as well as facilitate comparison to other previously published as well as future works, we consider a broad set of classification tasks from MoleculeNet that have been previously studied in the context of HDC and the SMILES-based encoding methods described in Section 4.3.1[27, 30]:

To facilitate comparison between our proposed methods, we follow the evaluation protocol previously proposed in MoleHD[27]. As in the case of MoleHD[27], we consider various splitting strategies that account for potential structural biases between the training and testing sets. This has become a standard practice after several studies pointed out the need to account for properties such as ligand structural similarity between training and testing sets that tends to inflate the values of relevant performance metrics [11, 30–32]. Unless otherwise stated, all algorithms described use the extended connectivity fingerprint extracted using the RDKit computational chemistry toolkit. We use the default parameters with 1024 bits and a radius of 2. The benchmark random forest (RF) and multilayer-perceptron (MLP) are implemented using the scikit-learn python machine learning toolkit. All sklearn-models have hyperparameter optimization using 10 samples of random search with $k = 5$ cross validation to choose optimal model hyperparameters. The best model is then instantiated and trained on the full training set. HDC models are trained using $D=10,000$ dimensional hypervector space with a maximum of 10 epochs for perceptron-style retraining. No further optimizations are performed. All HDC and scikit-learn (with optimal parameters) models are trained using 10 random seeds and all performance results are averaged over these seeds, error bars denote standard deviation over these runs.

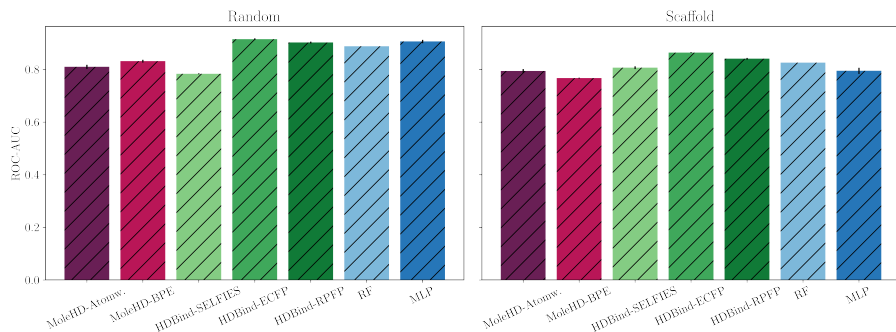


Fig. 1: Receiver Operation Curve for Blood-brain-barrier permeability evaluation. Each bar represents mean ROC-AUC score over 10 random seeds and the black vertical lines indicate the variance over the 10 seeds. All methods significantly outperform random. Our proposed ECFP based methods (HDBind-ECFP and HDBind-RFPF) strictly outperform the SMILES and SELFIES based HDC models and achieve competitive performance with the RF and MLP baselines on a random split of the data. The trend is also observed in the case of scaffold split where ligand similarity between the training and test sets is accounted for and minimized to some degree, suggesting the structural information present in the ECFP-based representations provides a representation the the HDC model is better able to generalize to new chemical space with.

In Figure 1 we give results for BBBP in conjunction with the random forest and multilayer perceptron (MLP) benchmark algorithms. In the case of randomly splitting the data into training and testing sets, our result in this case matches similar performance to previous state of the art results[30] and is better than random in terms of the receiver operating characteristic - area under the curve (ROC-AUC) score for all models considered. Similarly for the case of the chemical structure-informed scaffold splitting strategy, all models considered perform better than random by a significant margin. For random split, the worst HDC method still performs reasonably well considering the performance of the best model (RF) in terms of the ROC-AUC metric. Similarly, while all models perform worse on the scaffold split as expected, the gap in performance between the worst HDC model and the best baseline is not particularly large.

In Figure 2 we give results for the ClinTox dataset[30] using both random and scaffold splitting strategies. Models are trained according the previously described protocol. In the case of both train-test splitting strategies (random and scaffold), the SMILES string-based atomwise encoding method described by[27] outperforms all other methods. It is notable that the best previously reported SOA on this task (random split) was a text-based convolutional neural network (CNN). Across the board, our performance metrics in terms of the

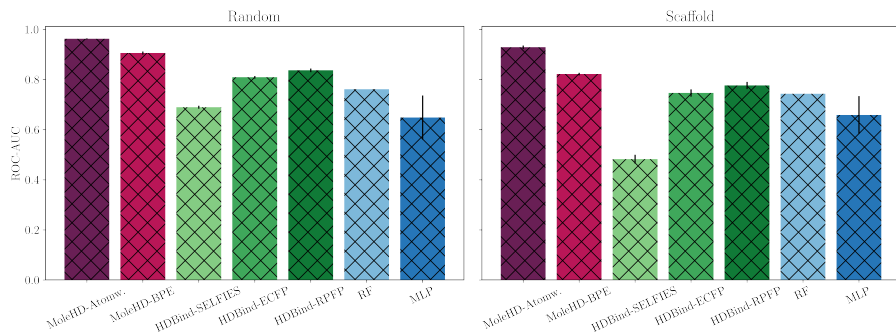
6 *HD-Bind*

Fig. 2: Barplots of ROC-AUC scores for the ClinTox dataset classification task of identification of FDA approved drugs. The MoleHD approaches in this case are strictly superior to all other HDC and baseline ML methods as well as the HDBind SELFIES encoding method. SMILES string based representations were previously demonstrated to achieve high performance on this task, thus this provides an additional sanity check on our approaches with a consistent observation in our specific context [30].

random split are similar to the performance previously reported[30]. Our metrics for the scaffold splitting strategy are similar (nearly consistently lower) however the MLP takes a dramatic hit in performance. This behavior is not surprising given the nature of MLP having significantly higher degrees of freedom than HDC-based approaches, thus making them prone to overfit on smaller datasets.

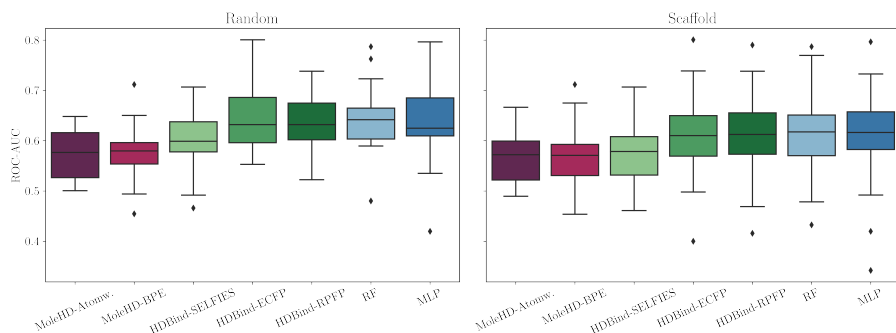


Fig. 3: Distributions of ROC-AUC scores over the 27 SIDER binary classification tasks. On random split and scaffold split, all models follow roughly the same order in terms of relative performance with slight increases in variance over the 27 tasks in the case of scaffold split. Our HDBind HDC approaches as well as the ECFP fingerprint trained baseline ML models consistently outperform the SELFIES and MoleHD SMILES based approaches.

Lastly for our MoleculeNet evaluation, we consider the SIDER dataset that includes 27 distinct binary classification tasks. We train each model separately for each task using the previously described protocol for hyperparameter optimization. Additionally we consider random and chemical structure-informed scaffold splitting strategies. In Figure 3 we show the performance of each method using the ROC-AUC metric to allow for comparison to previously reported state of the art results on these tasks. In each boxplot, we give the distribution of the ROC-AUC across the 27 distinct classification tasks for each method. In the case of both splitting strategies, our results are similar to those that have been previously reported with more advanced techniques[30]. Additionally, our novel ECFP-based encoding methods demonstrate a significant improve across both splits as compared to the SMILES-based methods previously reported in MoleHD[27].

2.2 DUD-E classification of Active and Inactive Molecules

Subsequently, we assess the viability of the HDC approaches on the task of distinguishing active versus decoy (inactive) ligands for a set of 38 protein targets collected from the Directory of Useful Decoys-Extended (DUD-E)[33]. This task requires one to develop a method that is able to identify “hit” molecules from a potentially large collection of candidates. While it has been shown that DUD-E exhibits a high degree of structural bias among the active and decoy molecules for each protein [31, 34], we consider this task as an additional sanity check for our approaches as it is well studied. DUD-E is also well known to be highly imbalanced, with the approximate ratio of actives to decoys being 1 : 50[33, 34].

We focus our analysis on alternative metrics that are more informative for the case of identifying hit compounds that may potentially be verified experimentally after using a computational protocol to select the most promising candidates from a large collection of molecules. In Figure 4 we give enrichment factor distributions over the 38 DUD-E human protein targets in our dataset. For each target a separate collection of active and decoy molecules are provided. We directly compare to previous work using the well known Vina scoring function within the LLNL-developed ConveyorLC HPC docking toolkit[2].

2.3 LIT-PCBA Challenge Dataset

In the practical setting, the number of actives for a given target will be significantly outnumbered by inactive molecules. A challenge with datasets such as DUD-E[33] is that while traditionally the set has served a role as the gold-standard benchmark for docking algorithms and other virtual screening methods including AI and deep learning-based, significant biases that have been demonstrated to over-inflate the performance of models have been identified[35–38]. Thus it has been the subject of much recent research in development of more challenging benchmark datasets to aid in the development of

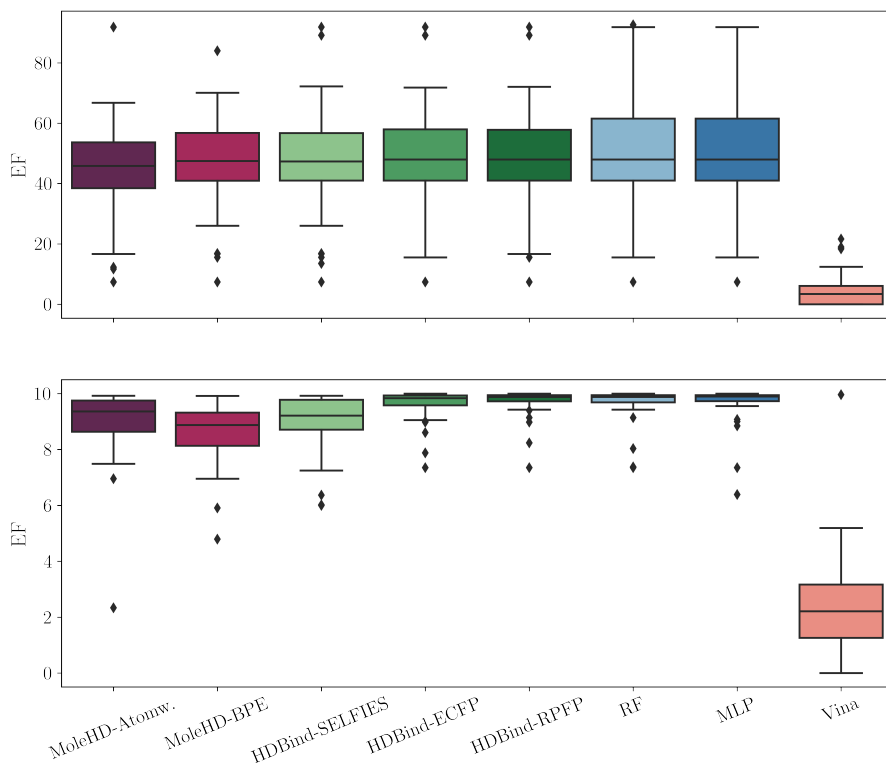


Fig. 4: Distributions of the enrichment metric are reported across all 38 DUD-E human protein targets. Results are reported as the average over 10 random seeds. (a) Enrichment at top 1% of screened library for DUD-E dataset. Nearly all models achieve the same median enrichment factor (approx. 46-48) and improve greatly upon the Vina molecular docking scoring function (3.4) (b) Enrichment at top 10% of screened library. Similarly, all models outperform Vina by a significant margin, demonstrating a consistent pattern of improvement. Vina achieves a median enrichment factor of 2.2 while the best HDC method achieves 9.9, competitive with the RF (9.9) and MLP (9.9) baselines. HDBind-ECFP and HDBind-RPPF are notably the better models in the case of (b) with considerably lower variance as compared to the MoleHD SMILES string based HDC methods.

more robust models[36]. The recently proposed LIT-PCBA[39] benchmark provides a rigorous test set that is more reflective of the true expected performance of the various predictive modeling techniques considered in virtual screening research. Subsequent studies of various techniques have been reported in the literature that clearly illustrates the challenges posed by this particular dataset[40, 41]. Our intent in reporting on this dataset is to test the limits of

our various approaches relative to each other as well as to what has been previously reported. We do not expect to outperform more sophisticated techniques as it is clear our motivation is in leveraging the clear computational efficiency possessed by our approaches with the goal being to achieve better than random performance. As this particular dataset is highly imbalanced, we elect not to report accuracy as it is highly uninformative in this setting. Rather we choose to report the *Receiver operating characteristic* or ROC which gives the true positive rate (TPR) as a function of the false positive rate (FPR), where the Area under the curve of a perfect classifier is the metric (ROC-AUC).

3 Discussion

We have demonstrated a range of methods for encoding molecular data for their use hardware-accelerated HDC-based classification methods. We demonstrated their relative performance on a number of representative classification tasks in the domain of molecular design and optimization of drug-like molecules. Future work will leverage the progress made in acceleration of HDC methods in hardware, leading to enormous gains in efficiency over state of the art neural network based approaches which require gradient-based training methods. The ability to rapidly train models with lightweight HDC-based approaches can enable more rapid exploration of the enormous drug-like chemical space. Further, the techniques proposed here can be adapted to other molecular optimization domains such as materials design. Our work can also extend to arbitrary molecular representations that can be learned with a neural network, thus allowing for HDC to co-exist as an efficient tool for subsequent training and inference stages. With more efficient use of available compute resources, the ecological impact of moving towards training and inference with lightweight methods can provide significant advantages over continued reliance on more expensive techniques.

Our results for HDC-based classification here are largely built upon the SMILES and ECFP representations, thus there may be great potential in leveraging ongoing research in molecular representation learning, notably in the context of Large Language Models (LLMs) such as ChemBERTa[42] and GPT-4[43]. Future work will investigate emerging representations that can potentially improve upon our predictive performance. Ideas from current research in attention mechanisms and transformer based architectures. Leveraging ongoing research in unsupervised learning and using these representations as the basis of our hypervectors. specifically learning these quantized representations in a deep learning architecture trained on large collections of molecules.

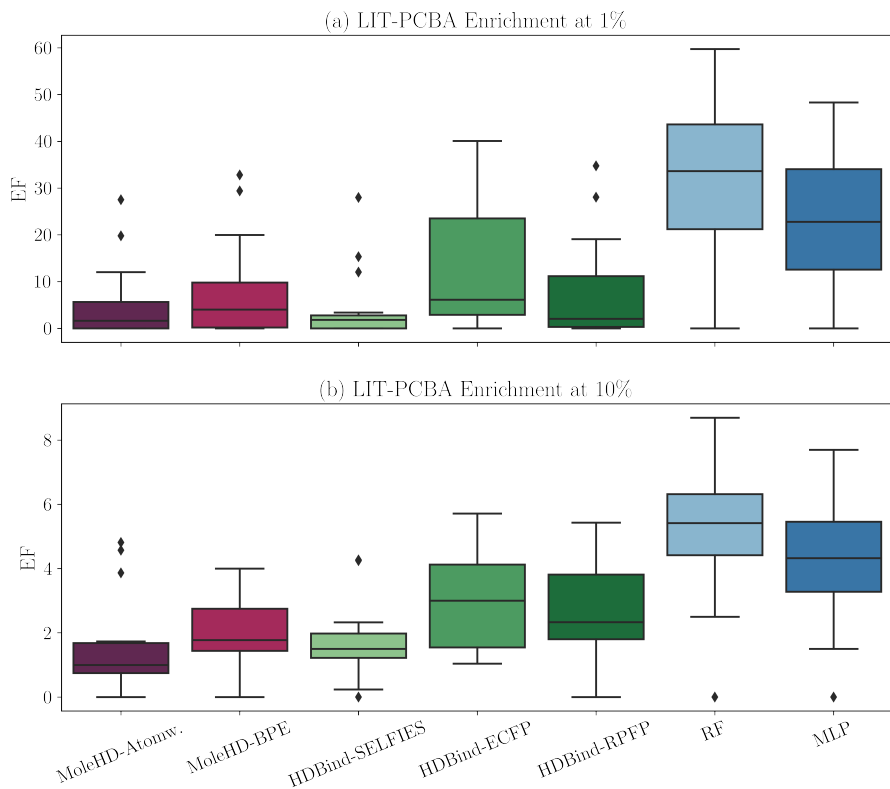


Fig. 5: Distributions are defined the enrichment metric are reported across all 15 protein targets and include agonists, inhibitors, and antagonists. Results are reported as the average over 10 random seeds. (a) Enrichment at top 1% of screened library for LIT-PCBA dataset. Both the RF and MLP strictly dominate the HDC-based methods in terms of enrichment factor metric (33.6 and 22.8 respectively) versus the best HDC method, HDBind-ECFP (6.1). (b) Enrichment at top 10% of screened library for LIT-PCBA dataset. The gap between the median enrichment factor between RF and MLP (5.4 and 4.3 respectively) is considerably smaller with the best HDC approach, HDBind-ECFP (3.0). In both cases, the best HDC approach is based upon our ECFP encoding methods.

4 Methods

4.1 Hyperdimensional Computing (HDC)

We briefly describe the HDC workflow that is depicted in Figure 6. At a high level, HDC works by relating an input “data-space” \mathcal{X} with an encoding dimension \mathcal{H} by way of a function $\phi : \mathcal{X} \rightarrow \mathcal{H}$. Formally, \mathcal{H} is defined as a real-valued inner-product space however in practice \mathcal{H} is usually restricted to be

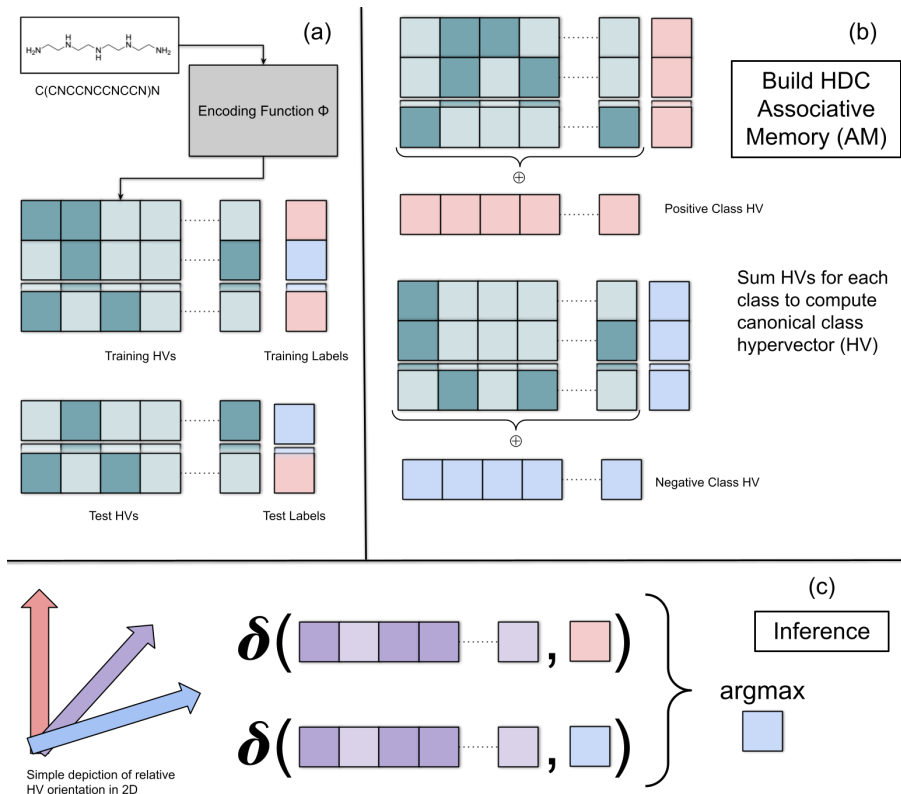


Fig. 6: Description of the HD computing paradigm. (a) The full set of components is given by some encoder that maps the raw input data to a high-dimensional space, the resulting set of hypervectors, and the corresponding labels. (b) Training or “building” the associative memory is formed for each of the k classes by bundling the hypervectors belonging to a given class into a canonical representation. (c) Inference is done by evaluating a similarity metric between a query hypervector and each of the canonical class representations stored in the associative memory, then assigning the class label that maximizes similarity to the query.

defined over integers in the range $[-b, b]$ where $b = 1$. Restricting to integers facilitates the acceleration of the method in hardware by using simpler arithmetic representations. Considering high-dimensional vector spaces for \mathcal{H} (e.g. $\{-1, 1\}^{10,000}$) results in useful properties gleaned from the “curse of dimensionality“. More specifically, in higher dimensional spaces, nearly all hypervectors are unrelated and can be considered as *quasi-orthogonal*, thus it is possible to assign semantically meaningful objects to unique hypervectors[18, 44]. Given the encodings of the data $h \in \mathcal{H}$ generated by ϕ , the h can then be manipulated using simple element-wise operators, “binding”, “bundling”, and permutation.

The bundling operator is defined as $\oplus : \mathcal{H} \times \mathcal{H} \rightarrow \mathcal{H}$, which maps a pair of hypervectors (h_i, h_j) to a new hypervector h_k that is similar to both, in our case we implement this as the element wise sum of the $\phi(x_i)$ in our dataset:

$$h = \phi(x) = \bigoplus_i^n \phi(x_i) \quad (1)$$

Thus, bundling allows for the composition of information from disparate sources into a single h .

The binding operator is used to create ordered tuples of points in \mathcal{H} and is defined as $\otimes : \mathcal{H} \times \mathcal{H} \rightarrow \mathcal{H}$. Binding is used to relate features to values and we specify it as:

$$h = \phi(x) = \bigoplus_{i=1}^n \psi(f_i) \otimes \phi(x_i) \quad (2)$$

Thus, binding can be used to build data structures such as the *item memory* (IM) which maps the possible alphabet symbols $a \in \mathcal{A}$ to unique hypervectors. Encoding then proceeds by mapping the input data point to a sequence of its constituent symbol hypervectors h_a , then aggregating these using a specific user-defined *encoding* protocol. We discuss the specific implementations of ϕ in Section 4.3.

4.2 Learning in HDC

The initial epoch of **training** or building the *Associative Memory* (i.e. AM) proceeds by *bundling* the hypervectors for each class k into h_k , producing a canonical representative vector (eq. 1) with a single pass of the training set. The subsequent **re-training** epochs refine the model by testing the prediction obtained for a given sample and updating h^k when the prediction is incorrect, analogous to the perceptron algorithm [18]. To perform **inference** on a query data point x^q we compute:

$$\hat{y} = \operatorname{argmax}_{k \in \{1, \dots, K\}} \langle h^k, \phi(x^q) \rangle \quad (3)$$

where $\langle \cdot, \cdot \rangle$ denotes a user specified similarity metric [18]. We opt to use the cosine similarity in order to compare h^q and h^k .

4.3 Encoding molecular data for HDC

4.3.1 MoleHD SMILES encoding

There are three approaches that we explore in context of the previous work MoleHD[27]; n -gram, atomwise, and SMILES-Pair Encoding[27, 45]. n -gram encoding assumes the existence of structure in the data where consecutive windows of the input string carry information regarding context in a sentence. The simplest form ($n = 1$ or uni-gram) treats each possible valid SMILES symbol

as an individual element in the encoding. Thus one smiles string of length n may at most have n unique symbols that represent it assuming no duplicates. However a limitation of this approach is exemplified by the fact “Cl” would be decomposed into “C” and “l”, resulting in an (incorrect) additional carbon atom and an invalid symbol in the representation. It is also possible that for arbitrary choices of n , additional artifacts may be introduced into the representation. We consider the cases of uni-gram ($n = 1$), bi-gram ($n = 2$), and tri-gram ($n = 3$). A simple improvement to the uni-gram algorithm instead treats atoms coherently as single symbols (e.g. “Cl” is treated as one symbol) can be called the *atom-level* encoding.

Recently, the SMILES Pair Encoding (SPE) was introduced to address limitations of the aforementioned encoding strategies. The SPE method is based on the “byte-pair encoding” (i.e. BPE)[46] that has become widely used in the NLP community, resulting in massive successes such as Dall-E 2[47]. SPE works by identifying high-frequency SMILES sub-strings in the atomwise representation (i.e. keep atoms coherent in tokens) and iteratively merging them in a bottom-up approach. SPE ensures that the most common sub-strings are assigned to unique tokens. Benefits of SPE are that it provides some ability to encode meaningful higher-level molecular substructures such as functional groups while also providing a compact representation that improves the computational efficiency of learning.

We study each of these sequence representations of smiles (char-level, atom-level, SPE) and use uni-gram ($n = 1$), bi-gram ($n = 2$), and tri-gram ($n = 3$) to further encode the strings in to an alphabet of symbols \mathcal{A} . Thus, for each input smiles string x_i , we iterate over each symbol and retrieve its h_a , then we shift the representation elements to the right by j position to encode the order information, then we add the result to the 0-initialized h_i describing x_i . The representation is then converted to a bipolarized binary representation where positive entries are mapped to 1 and entries less than or equal to 0 are mapped to -1. Learning then proceeds as described in Section 4.2. We implement our methods using the SmilesPE python package[45]. We found that the atomwise and SPE tokenizers consistently led to the best SMILES-based HDC models.

4.3.2 HDBind ECFP encoding

The ECFP representation of a molecule is widely used in computational chemistry for tasks such as similarity search in chemical libraries and in machine learning as features for prediction of a range of molecular-structure based predictive tasks. ECFP is based on the *Morgan algorithm*[48] (i.e. *MorganFP*) which was proposed to solve the molecular isomorphism problem. The MorganFP[48] algorithm represents the molecular structure explicitly as a graph where atoms are treated as nodes and covalent bonds are treated as edges. The ECFP algorithm makes changes to MorganFP that improve efficiency, such as using a user-defined iteration limit, using a cache to store intermediate atom identifiers between iterations, and a hashing scheme to record resulting representations encountered. Thus, ECFP effectively uses a

bottom-up approach to collect progressively larger molecular substructures that are guaranteed to preserve the graph structure and coherency. ECFP allows for a user to specify the number of bits in a representation, commonly chosen as 1024 or 2048. Further, a maximum radius size (i.e. number of bond “hops” from a root atom) for collecting substructure-graphs is specified. Thus, ECFP can be tweaked to allow for varying degree of resolution in the resultant representation.

In the case of ECFP representation, we take a similar approach to the SMILES based representation. The ECFP is made up of n -bits, with each value indicating the presence (bit=1) or lack thereof (bit=0) for a chemical substructure. While the SMILES representation allows for the different tokens to be specified in arbitrary order, the ECFP has a user-specified fixed number of bits. To compute the item memory (IM), we proceed by drawing random $(h_I, h_N) \in \{0, 1\}^D$ to represent the presence of a substructure h_I versus lack thereof h_N . We then draw random $h_p \in \{0, 1\}^D$ to represent the p -th position of the substructure. We then encode the x_i iterating over the bits indexed by j , selecting the value hypervector for position j and binding it with the position hypervector at index j . Our method can readily generalize to encode a larger dynamic range of values beyond the binary case, thus supporting ECFP count vectors, provided one is able to *a priori* specify the maximum count value.

4.3.3 HDBind Random projection fingerprint (RFPF) encoding

A simple encoding method is to use a random linear projection of the data into the HDC space:

$$h = \text{sign}(W^\top X) \quad (4)$$

where the weight matrix W is initialized according to a bernoulli distribution $p^k(1-p)^{1-k}$, where $p = 0.5$ and possible values lie within the set $\{0, 1\}$. Subsequently, the sample generated from the bernoulli distribution is transformed to a value in the set $\{-1, 1\}$ by multiplication by 2, then subtraction by 1. The bias term b is omitted (i.e. zero-valued vector). This encoding method allows for the mapping of a larger range of representation types as it lacks the restriction of a problem specific encoding alphabet. The viability of this approach remains yet unknown for encoding molecular representations.

4.3.4 HDBind SELFIES encoding

The SELFIES (SELF-referencing Embedded Strings) representation was recently proposed by [29] in order to address issues in chemical generative modeling tasks. SELFIES are defined by a formal grammar, a concept in theoretical computer science. A valid SELFIES corresponds to a valid molecule, a guarantee not provided by the SMILES representation. Additionally, SELFIES are able to handle supporting numerous constraints that are subject to ongoing research[49, 50]. However, it is not clear what representational advantages SELFIES possesses as compared to the SMILES representation beyond

chemical validity properties previously mentioned. We propose two straightforward encoding schemes for SELFIES that are somewhat analogous to the SMILES encoding presented in Section 4.3.1.

The first method simply tokenizes a SELFIES string into the individual characters present, mapping each of the unique characters to a corresponding randomly drawn binary hypervector of dimension D . Next, we bundle the character hypervectors present in a given molecules SELFIES to form the molecule hypervector. The second method instead only tokenizes the unique SELFIES terminals present in a given string. Similarly to the previous method, the unique terminals are mapped to corresponding randomly drawn binary hypervectors. Subsequently we bundle the together the terminal hypervectors present in a given SELFIES to form the molecule hypervector.

4.4 Metrics

We employ a variety of metrics to assess the classification performance of our HD-based methods that go beyond simply measuring accuracy. This is particularly important in the domain of virtual screening as the class distributions are significantly different in terms of size. To facilitate comparison with previous work on the MoleculeNet suite of molecular machine learning benchmarking datasets[30] which uses the Reciever Operating Characteristic - Area Under the Curve (ROC-AUC) to measure performance between different models. ROC-AUC is defined by computing the True Positive Rate (TPR) as a function of the False Positive Rate (FPR), defined in equations 6 and 5, at different thresholds of a classifiers score (e.g. probability of being positive class).

$$\text{TPR} = \frac{TP}{TP + FN} \quad (5)$$

$$\text{FPR} = \frac{FP}{FP + TN} \quad (6)$$

In the domain of drug discovery, it is also common to encounter the Enrichment Factor (EF) metric[9, 51], which attempts to measure how well a screening method may be able to improve the density of actives in a large database of molecular candidates. While this metric does not require a screening method to necessarily be as accurate as other more expensive methods, it does favor methods that are able to reliably *rank* molecules in such a way that it becomes more likely to draw a successful candidate after a set has been filtered. Being able to improve the speed at which this can be done also invites the possibility of pushing the boundaries in terms of number of initial candidates that can be considered. Following the work of [2], we define the EF as:

$$\text{EF}^{\%} = \frac{\text{actives}_{\text{sampled}}}{\text{actives}_{\text{total}}} \frac{N_{\text{total}}}{N_{\text{sampled}}} \quad (7)$$

where $\text{actives}_{\text{sampled}}$ is the number of actives in a sample at $X\%$ of the database, $\text{actives}_{\text{total}}$ is the total number of actives in the database, N_{total} is the total size of the database, and N_{sampled} is the size of the sample at $X\%$ of the database.

We use the equation introduced in MoleHD[27] to measure the similarity of a query hypervector h_q to the active class hypervector h_a in order to compute a measure that can be used to sort compounds to approximate likelihood of binding.

$$\eta = \frac{1}{2} + \frac{1}{4}(\delta(h_q, h_a) - \delta(h_q, h_i)) \quad (8)$$

4.5 HDC acceleration

We compare the speed of performing docking on the DUD-E dataset[2], in terms of a single compound, and compare to performing inference for binding activity using HDC. According to previous work on the same set of 38 protein targets, performing a screen for a target with approximately 4,000 atoms against a library of 40,000 molecules would require approximately 1 month or a total of 2.628×10^6 seconds to screen (approximately 65.7 seconds per molecule) on a single CPU and approximately 1 hour (3600 seconds / 40000 molecules = .09 seconds per molecule) on 700 CPUs [2].

$$t_s = \frac{t_{\text{baseline}}}{t_{\text{model}}} \quad (9)$$

In table 1 we give the latency (in seconds) to compute inference on the average molecule from the DUD-E dataset we consider in this work. Specifically, the average test time for each model is divided by the average number of molecules in each of the 38 target test sets to arrive at the latency per molecule estimate. We compute the speedup according to equation 9.

4.6 Computer Hardware Specifications

All models are run on in the same hardware environment, namely the Pascal GPU cluster at Lawrence Livermore National Laboratory. All models were run on a single node of Pascal. A Pascal node features 2x NVIDIA P100 GPUs, an Intel Xeon E5-2695v4 CPUs with 36 physical cores, and 256GB of main memory.

Method	Median Latency (per molecule (s))	Speedup
RF	2.78×10^{-5}	-
MLP	1.04×10^{-5}	2.68
MoleHD-Atomwise	3.79×10^{-7}	73.39
MoleHD-BPE	4.10×10^{-7}	67.89
HDBind-Selfies	3.07×10^{-7}	90.57
HDBind-ECFP	3.80×10^{-7}	73.18
HDBind-RPFP	3.50×10^{-7}	79.37

Table 1: Inference comparison on DUD-E benchmark dataset. Measured latency for AutoDock Vina is 22.3 seconds per molecule, demonstrating the dramatic efficiency improvement for each ML and HDC method considered in our work. Speedup in this case is measured according to the slowest ML model, the Random Forest (RF). All HDC methods (MoleHD and HDBind) significantly outperform the baseline ML methods.

4.7 Sci-kit Learn Training and Parameter Selection

Sci-kit learn was used for the implementation of the Multilayer Perceptron (MLP) and Random Forest baseline approaches. Our goal was not to exhaustively search parameter space to find an optimal model, rather to use a lightweight routine to find a simple yet reasonable model. We use random search for hyperparameter optimization, using 10 samples of hyperparameters along with 5 fold cross validation for a total of 50 fits per model per classification task.

Acknowledgments. This work was supported in part by CRISP, one of six centers in JUMP, an SRC program sponsored by DARPA. This work was performed under the auspices of the U.S. Department of Energy by Lawrence Livermore National Laboratory under Contract DE-AC52-07NA27344, LLNLJRN-ABCXYZ. We thank Michael K. Gilson, Rose Yu, and Stewart He for their helpful feedback in the development of this work.

References

- [1] Burt, J., Morgan, T.P.: Top 500 - The List. <https://www.top500.org/>. Accessed: 2022-12-30
- [2] Zhang, X., Wong, S.E., Lightstone, F.C.: Toward fully automated high performance computing drug discovery: a massively parallel virtual screening pipeline for docking and molecular mechanics/generalized born surface area rescoring to improve enrichment. *J. Chem. Inf. Model.* **54**(1), 324–337 (2014)
- [3] Trott, O., Olson, A.J.: AutoDock vina: improving the speed and accuracy of docking with a new scoring function, efficient optimization, and multithreading. *J. Comput. Chem.* **31**(2), 455–461 (2010)

- [4] Eberhardt, J., Santos-Martins, D., Tillack, A.F., Forli, S.: AutoDock vina 1.2.0: New docking methods, expanded force field, and python bindings. *J. Chem. Inf. Model.* **61**(8), 3891–3898 (2021)
- [5] Massova, I., Kollman, P.A.: Combined molecular mechanical and continuum solvent approach (MM-PBSA/GBSA) to predict ligand binding. *Perspect. Drug Discov. Des.* **18**(1), 113–135 (2000)
- [6] Greenidge, P.A., Kramer, C., Mozziconacci, J.-C., Wolf, R.M.: MM/G-BSA binding energy prediction on the PDBbind data set: successes, failures, and directions for further improvement. *J. Chem. Inf. Model.* **53**(1), 201–209 (2013)
- [7] Wright, D.W., Hall, B.A., Kenway, O.A., Jha, S., Coveney, P.V.: Computing clinically relevant binding free energies of HIV-1 protease inhibitors. *J. Chem. Theory Comput.* **10**(3), 1228–1241 (2014)
- [8] Lau, E.Y., Negrete, O.A., Bennett, W.F.D., Bennion, B.J., Borucki, M., Bourguet, F., Epstein, A., Franco, M., Harmon, B., He, S., Jones, D., Kim, H., Kirshner, D., Lao, V., Lo, J., McLoughlin, K., Mosesso, R., Muruges, D.K., Saada, E.A., Segelke, B., Stefan, M.A., Stevenson, G.A., Torres, M.W., Weilhammer, D.R., Wong, S., Yang, Y., Zemla, A., Zhang, X., Zhu, F., Allen, J.E., Lightstone, F.C.: Discovery of Small-Molecule inhibitors of SARS-CoV-2 proteins using a computational and experimental pipeline. *Front Mol Biosci* **8**, 678701 (2021)
- [9] Gentile, F., Agrawal, V., Hsing, M., Ton, A.-T., Ban, F., Norinder, U., Gleave, M.E., Cherkasov, A.: Deep docking: A deep learning platform for augmentation of structure based drug discovery. *ACS Cent Sci* **6**(6), 939–949 (2020)
- [10] Clyde, A., Liu, X., Brettin, T., Yoo, H., Partin, A., Babuji, Y., Blaiszik, B., Mohd-Yusof, J., Merzky, A., Turilli, M., Jha, S., Ramanathan, A., Stevens, R.: AI-accelerated protein-ligand docking for SARS-CoV-2 is 100-fold faster with no significant change in detection. *Sci. Rep.* **13**(1), 2105 (2023)
- [11] Jones, D., Kim, H., Zhang, X., Zemla, A., Stevenson, G., Bennett, W.F.D., Kirshner, D., Wong, S.E., Lightstone, F.C., Allen, J.E.: Improved Protein-Ligand binding affinity prediction with Structure-Based deep fusion inference. *J. Chem. Inf. Model.* **61**(4), 1583–1592 (2021)
- [12] Jiménez, J., Škalič, M., Martínez-Rosell, G., De Fabritiis, G.: KDEEP: Protein–Ligand absolute binding affinity prediction via 3D-Convolutional neural networks. *J. Chem. Inf. Model.* **58**(2), 287–296 (2018)

- [13] Stepniewska-Dziubinska, M.M., Zielenkiewicz, P., Siedlecki, P.: Development and evaluation of a deep learning model for protein-ligand binding affinity prediction. *Bioinformatics* **34**(21), 3666–3674 (2018)
- [14] Stevenson, G.A., Jones, D., Kim, H., Bennett, W.F.D., Bennion, B.J., Borucki, M., Bourguet, F., Epstein, A., Franco, M., Harmon, B., He, S., Katz, M.P., Kirshner, D., Lao, V., Lau, E.Y., Lo, J., McLoughlin, K., Mosesso, R., Muruges, D.K., Negrete, O.A., Saada, E.A., Segelke, B., Stefan, M., Torres, M.W., Weilhammer, D., Wong, S., Yang, Y., Zemla, A., Zhang, X., Zhu, F., Lightstone, F.C., Allen, J.E.: High-throughput virtual screening of small molecule inhibitors for SARS-CoV-2 protein targets with deep fusion models. In: Proceedings of the International Conference for High Performance Computing, Networking, Storage and Analysis. SC '21, pp. 1–13. Association for Computing Machinery, New York, NY, USA (2021)
- [15] Jacobs, S.A., Moon, T., McLoughlin, K., Jones, D., Hysom, D., Ahn, D.H., Gyllenhaal, J., Watson, P., Lightstone, F.C., Allen, J.E., Karlin, I., Van Essen, B.: Enabling rapid COVID-19 small molecule drug design through scalable deep learning of generative models. *Int. J. High Perform. Comput. Appl.* **35**(5), 469–482 (2021)
- [16] Plate, T.A.: Holographic reduced representations. *IEEE Trans. Neural Netw.* **6**(3), 623–641 (1995)
- [17] Kanerva, P.: Hyperdimensional computing: An introduction to computing in distributed representation with high-dimensional random vectors. *Cognit. Comput.* **1**(2), 139–159 (2009)
- [18] Thomas, A., Dasgupta, S., Rosing, T.: A theoretical perspective on hyperdimensional computing. *J. Artif. Intell. Res.* **72**, 215–249 (2021)
- [19] Karunaratne, G., Le Gallo, M., Cherubini, G., Benini, L., Rahimi, A., Sebastian, A.: In-memory hyperdimensional computing (2019) <https://arxiv.org/abs/1906.01548> [cs.ET]
- [20] Ge, L., Parhi, K.K.: Classification using hyperdimensional computing: A review. *IEEE Circuits and Systems Magazine* **20**(2), 30–47 (2020)
- [21] Rahimi, A., Kanerva, P., Benini, L., Rabaey, J.M.: Efficient biosignal processing using hyperdimensional computing: Network templates for combined learning and classification of ExG signals. *Proc. IEEE* **107**(1), 123–143 (2019)
- [22] Burrello, A., Cavigelli, L., Schindler, K., Benini, L., Rahimi, A.: Laelaps: An Energy-Efficient seizure detection algorithm from long-term human iEEG recordings without false alarms. In: 2019 Design, Automation Test

- in Europe Conference Exhibition (DATE), pp. 752–757 (2019)
- [23] Rasanen, O.J., Saarinen, J.P.: Sequence prediction with sparse distributed hyperdimensional coding applied to the analysis of mobile phone use patterns. *IEEE Trans Neural Netw Learn Syst* **27**(9), 1878–1889 (2016)
- [24] Mitrokhin, A., Sutor, P., Fermüller, C., Aloimonos, Y.: Learning sensorimotor control with neuromorphic sensors: Toward hyperdimensional active perception. *Sci Robot* **4**(30) (2019)
- [25] Kanerva, P., Kristoferson, J., Holst, A.: Random indexing of text samples for latent semantic analysis. In: *Proceedings of the Annual Meeting of the Cognitive Science Society*, vol. 22 (2000)
- [26] Kang, J., Khaleghi, B., Kim, Y., Rosing, T.: Xcelhd: An efficient gpu-powered hyperdimensional computing with parallelized training. *The 27th Asia and South Pacific Design Automation Conference* (2022)
- [27] Ma, D., Thapa, R., Jiao, X.: MoleHD: Efficient drug discovery using brain inspired hyperdimensional computing. In: *2022 IEEE International Conference on Bioinformatics and Biomedicine (BIBM)*, pp. 390–393 (2022)
- [28] Rogers, D., Hahn, M.: Extended-connectivity fingerprints. *J. Chem. Inf. Model.* **50**(5), 742–754 (2010)
- [29] Krenn, M., Häse, F., Nigam, A., Friederich, P., Aspuru-Guzik, A.: Self-referencing embedded strings (SELFIES): A 100% robust molecular string representation. *Mach. Learn. Sci. Technol.* **1**(4), 045024 (2020)
- [30] Wu, Z., Ramsundar, B., Feinberg, E.N., Gomes, J., Geniesse, C., Pappu, A.S., Leswing, K., Pande, V.: MoleculeNet: a benchmark for molecular machine learning. *Chem. Sci.* **9**(2), 513–530 (2018)
- [31] Ellingson, S.R., Davis, B., Allen, J.: Machine learning and ligand binding predictions: A review of data, methods, and obstacles. *Biochim. Biophys. Acta Gen. Subj.* **1864**(6), 129545 (2020)
- [32] Feinberg, E.N., Sur, D., Wu, Z., Husic, B.E., Mai, H., Li, Y., Sun, S., Yang, J., Ramsundar, B., Pande, V.S.: PotentialNet for molecular property prediction. *ACS Cent Sci* **4**(11), 1520–1530 (2018)
- [33] Mysinger, M.M., Carchia, M., Irwin, J.J., Shoichet, B.K.: Directory of useful decoys, enhanced (DUD-E): better ligands and decoys for better benchmarking. *J. Med. Chem.* **55**(14), 6582–6594 (2012)
- [34] Jones, D., Bopaiah, J., Alghamedy, F., Jacobs, N., Weiss, H.L., de

- Jong, W.A., Ellingson, S.R.: Polypharmacology within the full kinome: a machine learning approach. *AMIA Jt Summits Transl Sci Proc* **2017**, 98–107 (2018)
- [35] Chaput, L., Martinez-Sanz, J., Saettel, N., Mouawad, L.: Benchmark of four popular virtual screening programs: construction of the active/decoy dataset remains a major determinant of measured performance. *J. Cheminform.* **8**, 56 (2016)
- [36] Wallach, I., Heifets, A.: Most Ligand-Based classification benchmarks reward memorization rather than generalization. *J. Chem. Inf. Model.* **58**(5), 916–932 (2018)
- [37] Chen, L., Cruz, A., Ramsey, S., Dickson, C.J., Duca, J.S., Hornak, V., Koes, D.R., Kurtzman, T.: Hidden bias in the DUD-E dataset leads to misleading performance of deep learning in structure-based virtual screening. *PLoS One* **14**(8), 0220113 (2019)
- [38] Sieg, J., Flachsenberg, F., Rarey, M.: In need of bias control: Evaluating chemical data for machine learning in Structure-Based virtual screening. *J. Chem. Inf. Model.* **59**(3), 947–961 (2019)
- [39] Tran-Nguyen, V.-K., Jacquemard, C., Rognan, D.: LIT-PCBA: An unbiased data set for machine learning and virtual screening. *J. Chem. Inf. Model.* (2020)
- [40] Jiang, D., Hsieh, C.-Y., Wu, Z., Kang, Y., Wang, J., Wang, E., Liao, B., Shen, C., Xu, L., Wu, J., Cao, D., Hou, T.: InteractionGraphNet: A novel and efficient deep graph representation learning framework for accurate Protein-Ligand interaction predictions. *J. Med. Chem.* **64**(24), 18209–18232 (2021)
- [41] Tran-Nguyen, V.-K., Bret, G., Rognan, D.: True accuracy of fast scoring functions to predict High-Throughput screening data from docking poses: The simpler the better. *J. Chem. Inf. Model.* **61**(6), 2788–2797 (2021)
- [42] Chithrananda, S., Grand, G., Ramsundar, B.: ChemBERTa: Large-Scale Self-Supervised pretraining for molecular property prediction (2020) <https://arxiv.org/abs/2010.09885> [cs.LG]
- [43] OpenAI: GPT-4 technical report (2023) <https://arxiv.org/abs/2303.08774> [cs.CL]
- [44] Yu, T., Zhang, Y., Zhang, Z., De Sa, C.: Understanding hyperdimensional computing for parallel Single-Pass learning (2022) <https://arxiv.org/abs/2202.04805> [cs.LG]

- [45] Li, X., Fourches, D.: SMILES pair encoding: A Data-Driven substructure tokenization algorithm for deep learning. *J. Chem. Inf. Model.* **61**(4), 1560–1569 (2021)
- [46] Sennrich, R., Haddow, B., Birch, A.: Neural machine translation of rare words with subword units. In: Proceedings of the 54th Annual Meeting of the Association for Computational Linguistics (Volume 1: Long Papers), pp. 1715–1725. Association for Computational Linguistics, Berlin, Germany (2016)
- [47] Ramesh, A., Dhariwal, P., Nichol, A., Chu, C., Chen, M.: Hierarchical Text-Conditional image generation with CLIP latents (2022) <https://arxiv.org/abs/2204.06125> [cs.CV]
- [48] Morgan, H.L.: The generation of a unique machine description for chemical Structures-A technique developed at chemical abstracts service. *J. Chem. Doc.* **5**(2), 107–113 (1965)
- [49] Krenn, M., Ai, Q., Barthel, S., Carson, N., Frei, A., Frey, N.C., Friederich, P., Gaudin, T., Gayle, A.A., Jablonka, K.M., Lameiro, R.F., Lemm, D., Lo, A., Moosavi, S.M., Nápoles-Duarte, J.M., Nigam, A., Pollice, R., Rajan, K., Schatzschneider, U., Schwaller, P., Skreta, M., Smit, B., Strieth-Kalthoff, F., Sun, C., Tom, G., Falk von Rudorff, G., Wang, A., White, A.D., Young, A., Yu, R., Aspuru-Guzik, A.: SELFIES and the future of molecular string representations. *Patterns (N Y)* **3**(10), 100588 (2022)
- [50] Lo, A., Pollice, R., Nigam, A., White, A.D., Krenn, M., Aspuru-Guzik, A.: Recent advances in the Self-Referencing embedding strings (SELFIES) library (2023) <https://arxiv.org/abs/2302.03620> [physics.chem-ph]
- [51] Bender, A., Glen, R.C.: A discussion of measures of enrichment in virtual screening: comparing the information content of descriptors with increasing levels of sophistication. *J. Chem. Inf. Model.* **45**(5), 1369–1375 (2005)